Properties of "pasta" phases in neutron stars

Hoa DINH THI, Anthea FANTINA, Francesca GULMINELLI

June 20 - 24, 2022

Neutron stars as multi-messenger laboratories for dense matter

UNIVERSITÉ CAEN NORMANDIE

laboratoire commun CEA/DRF CNRS/IN2P3

laboratoire de physique corpusculaire

1. Pasta phase in neutrons stars

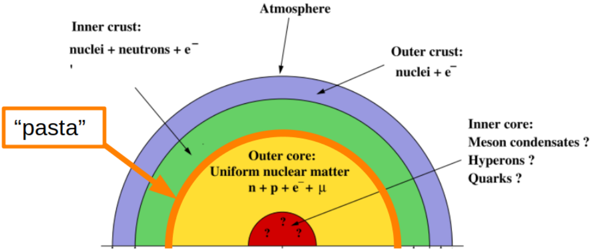

$\rightarrow$ **Pasta phase** is expected to exist at the bottom of the **inner crust**, before the transition to the **core**.

Original figure taken from Fiorella Burgio, G.; Vidana, I. Universe 2020, 6(8), 119

2. Different shapes in the pasta phase

- 5 phases: spheres, rods, slabs, tubes, bubbles
  "inverted" configurations

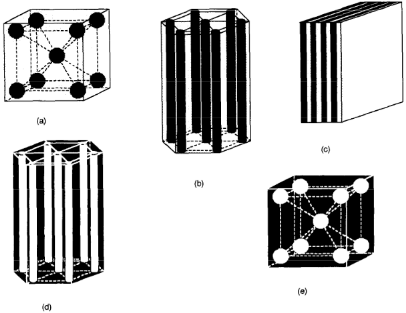

Ravenhall et al., Phys. Rev. Lett. 27, 2066 (1983)
Hashimoto et al., Prog. Theor. Phys. 71, 320 (1984)
K. Oyamatsu, Nucl. Phys. A561, 431 (1993)

3. Formalism

Compressible **L**iquid **D**rop **M**odel (Carreau et al.):

$$\Omega = n_p m_p c^2 + (n_B - n_p) m_n c^2$$
$$+ n_0 e_{HM}(n_0, I)\mathsf{f} + \epsilon_{surf} + \epsilon_{curv} + \epsilon_{Coul}$$
$$+ n_g e_{HM}(n_g, 1)(1 - \mathsf{f}) + \epsilon_e - \mu n_B.$$

Compressible **L**iquid **D**rop **M**odel (Carreau et al.):

$$\Omega = n_p m_p c^2 + (n_B - n_p) m_n c^2 + n_0 e_{HM}(n_0, I)\mathsf{f} + \epsilon_{surf} + \epsilon_{curv} + \epsilon_{Coul} + n_g e_{HM}(n_g, 1)(1 - \mathsf{f}) + \epsilon_e - \mu n_B .$$

Compressible **L**iquid **D**rop **M**odel (Carreau et al.):

$$\Omega = n_p m_p c^2 + (n_B - n_p) m_n c^2$$
$$+ \; n_0 e_{HM}(n_0, I)\mathsf{f} + \epsilon_{surf} + \epsilon_{curv} + \epsilon_{Coul}$$
$$+ \; n_g e_{HM}(n_g, 1)(1 - \mathsf{f}) + \epsilon_e - \mu n_B .$$

3. Formalism

Compressible **L**iquid **D**rop **M**odel (Carreau et al.):

$$\Omega = n_p m_p c^2 + (n_B - n_p) m_n c^2 + n_0 e_{HM}(n_0, I)\mathsf{f} + \epsilon_{surf} + \epsilon_{curv} + \epsilon_{Coul} + n_g e_{HM}(n_g, 1)(1 - \mathsf{f}) + \epsilon_e - \mu n_B.$$

3. Formalism

Compressible **L**iquid **D**rop **M**odel (Carreau et al.):

$$\Omega = n_p m_p c^2 + (n_B - n_p) m_n c^2 + n_0 e_{HM}(n_0, I)\mathsf{f} + \epsilon_{surf} + \epsilon_{curv} + \epsilon_{Coul} + n_g e_{HM}(n_g, 1)(1 - \mathsf{f}) + \epsilon_e - \mu n_B .$$

3. Formalism

Compressible **L**iquid **D**rop **M**odel (Carreau et al.):

$$\Omega = n_p m_p c^2 + (n_B - n_p) m_n c^2 + n_0\, e_{HM}(n_0, I)\, \mathrm{f} + \epsilon_{surf} + \epsilon_{curv} + \epsilon_{Coul} + n_g e_{HM}(n_g, 1)(1 - \mathrm{f}) + \epsilon_e - \mu n_B.$$

- Bulk energy, $e_{HM}(n, \delta)$), is calculated using the **meta-modeling** technique.

3. Formalism

Compressible **L**iquid **D**rop **M**odel (Carreau et al.):

$$\Omega = n_p m_p c^2 + (n_B - n_p) m_n c^2$$
$$+ n_0 \, e_{HM}(n_0, I) \, \mathsf{f} + \epsilon_{surf} + \epsilon_{curv} + \epsilon_{Coul}$$
$$+ n_g e_{HM}(n_g, 1)(1 - \mathsf{f}) + \epsilon_e - \mu n_B .$$

- Bulk energy, $e_{HM}(n, \delta))$, is calculated using the **meta-modeling** technique.
  $\rightarrow$ 13 **bulk** parameters: $E_{sat/sym}$, n_{sat}, L_{sym}, $K_{sat/sym}$, ...
  Margueron et al. Phys. Rev. C, 97:025806, 2018

3. Formalism

Compressible **L**iquid **D**rop **M**odel (Carreau et al.):

$$\Omega = n_p m_p c^2 + (n_B - n_p) m_n c^2 + n_0 \, e_{HM}(n_0, I) \, \mathrm{f} + \epsilon_{surf} + \epsilon_{curv} + \epsilon_{Coul} + n_g e_{HM}(n_g, 1)(1 - \mathrm{f}) + \epsilon_e - \mu n_B .$$

- Bulk energy, $e_{HM}(n, \delta))$, is calculated using the **meta-modeling** technique.
  $\rightarrow$ 13 **bulk** parameters: $E_{sat/sym}$, n_{sat}, L_{sym}, $K_{sat/sym}$, ...
  Margueron et al. Phys. Rev. C, 97:025806, 2018
- Surface, curvature, and Coulomb energies depend on nuclear shape. $\rightarrow$ 5 surface parameters: σ_0, $\sigma_{0,c}$, β, b_s, p

Equilibrium configuration

- **Step 1**: Minimizing Ω for each geometry

Equilibrium configuration

- **Step 1**: Minimizing Ω for each geometry
  $\rightarrow$ composition (n_p, I, n_0, n_g, r_N)

Equilibrium configuration

- **Step 1**: Minimizing Ω for each geometry
  $\rightarrow$ composition (n_p, I, n_0, n_g, r_N) + energy density.

Equilibrium configuration

- **Step 1**: Minimizing Ω for each geometry
  $\rightarrow$ composition (n_p, I, n_0, n_g, r_N) + energy density.
- **Step 2**: Comparing energy densities among all geometries
  $\rightarrow$ equilibrium geometry.

4. Model dependence of pasta-phase properties

Equilibrium geometries

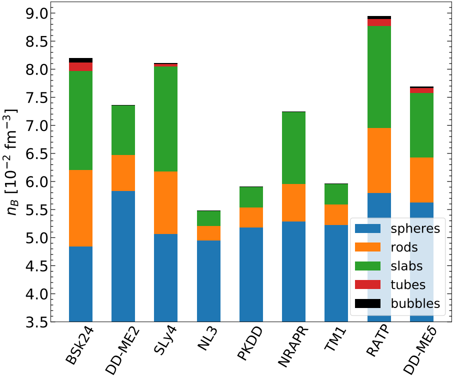

4. Model dependence of pasta-phase properties

Equilibrium geometries

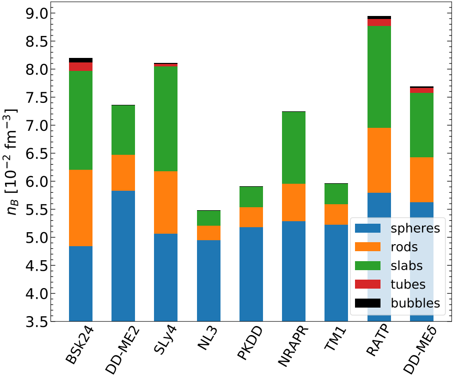

Proton fraction $y_p = Z/A$

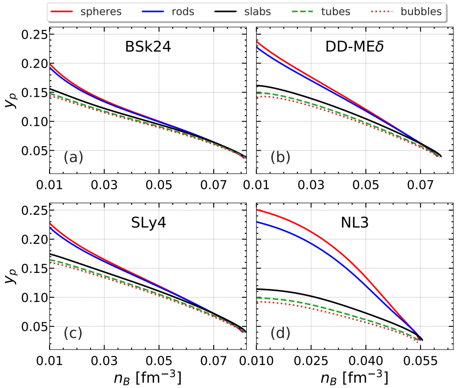

4. Model dependence of pasta-phase properties

Equilibrium geometries

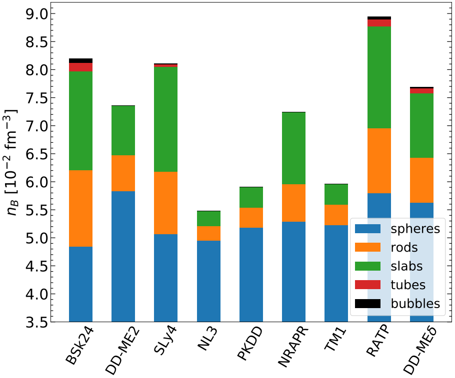

Proton fraction $y_p = Z/A$

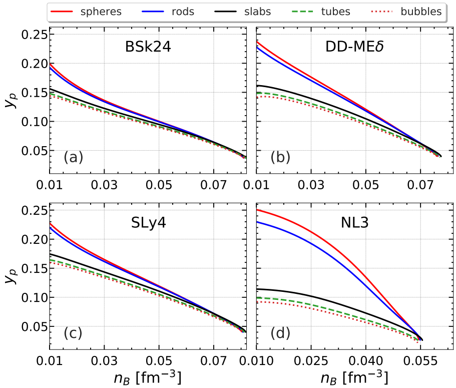

- Properties of pasta phases are model dependent.

4. Model dependence of pasta-phase properties

Equilibrium geometries

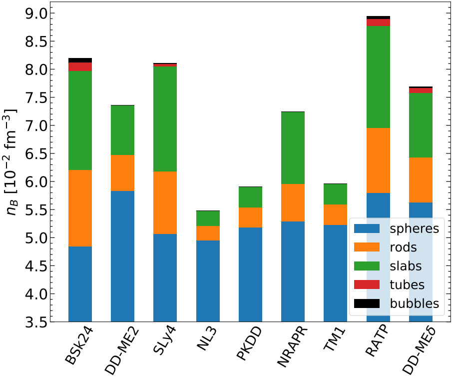

Proton fraction $y_p = Z/A$

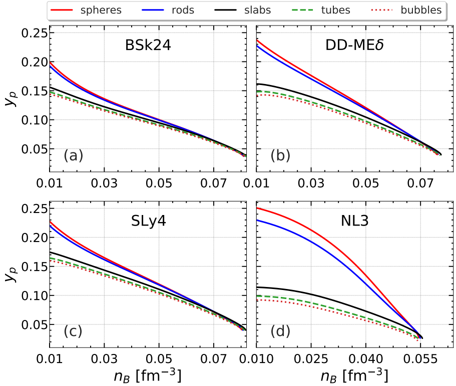

- Properties of pasta phases are model dependent.
- Use Bayesian analysis to study the influence of energy functional on the uncertainties of pasta-phase properties.

Dinh Thi, H., et al. . Eur. Phys. J. A 57, 296 (2021)

5. Bayesian analysis

Bayes' theorem

$$P(\{X\}|\mathbf{c}) = \mathcal{N} P_{prior}(\{X\}) \prod_k P(c_k|\{X\})$$

5. Bayesian analysis

Bayes' theorem

$$P(\{X\}|\mathbf{c}) = \mathcal{N} P_{prior}(\{X\}) \prod_k P(c_k|\{X\})$$

Prior

- Bulk parameters $\{X\}$:

Parameters	Min	Max
E_{sat} (MeV)	-17	-15
n_{sat} (fm^{-3})	0.15	0.17
K_{sat} (MeV)	190	270
Q_{sat} (MeV)	-1000	1000
Z_{sat} (MeV)	-3000	3000
E_{sym} (MeV)	26	38
L_{sym} (MeV)	10	80
K_{sym} (MeV)	-400	200
Q_{sym} (MeV)	-2000	2000
Z_{sym} (MeV)	-5000	5000
$m^{\star}_{sat}/m$	0.6	0.8
$\Delta m^{\star}_{sat}/m$	0.0	0.2
b	1	6
p	2	4

Margueron et al. Phys. Rev. C 2018, 97:025806

5. Bayesian analysis

Bayes' theorem

$$P(\{X\}|\mathbf{c}) = \mathcal{N} P_{prior}(\{X\}) \prod_k P(c_k|\{X\})$$

Prior

- Bulk parameters $\{X\}$:

Parameters	Min	Max
E_{sat} (MeV)	-17	-15
n_{sat} (fm^{-3})	0.15	0.17
K_{sat} (MeV)	190	270
Q_{sat} (MeV)	-1000	1000
Z_{sat} (MeV)	-3000	3000
E_{sym} (MeV)	26	38
L_{sym} (MeV)	10	80
K_{sym} (MeV)	-400	200
Q_{sym} (MeV)	-2000	2000
Z_{sym} (MeV)	-5000	5000
$m^{\star}_{sat}/m$	0.6	0.8
$\Delta m^{\star}_{sat}/m$	0.0	0.2
b	1	6
p	2	4

Margueron et al. Phys. Rev. C 2018, 97:025806

- Surface and curvature parameters: $\{\sigma_0, b_s, \sigma_{0c}, \beta\}$.

  Fit to AME2016 mass table:

$$p_{AME}(\{X\}) = e^{-\chi^2(\{X\})/2}$$

Huang et al. Chin. Phys. C 2017, 41, 03000

5. Bayesian analysis

Posterior: obtained by applying 2 constraints on the prior.

Posterior: obtained by applying 2 constraints on the prior.

1. Low density (LD) filter (Drischler et al., Phys. Rev. C, 93, 054314, 2016):

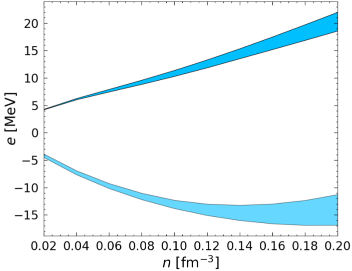

5. Bayesian analysis

Posterior: obtained by applying 2 constraints on the prior.

1. Low density (LD) filter (Drischler et al., Phys. Rev. C, 93, 054314, 2016):

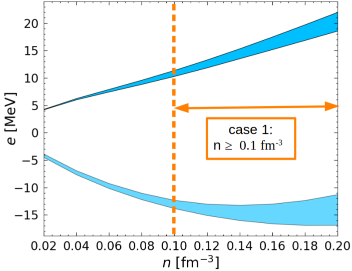

5. Bayesian analysis

Posterior: obtained by applying 2 constraints on the prior.

1. Low density (LD) filter (Drischler et al., Phys. Rev. C, 93, 054314, 2016):

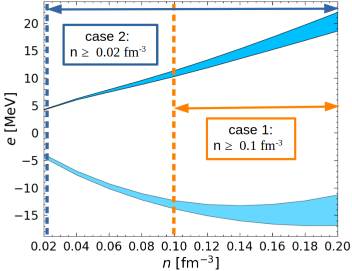

Posterior: obtained by applying 2 constraints on the prior.

1. Low density (LD) filter (Drischler et al., Phys. Rev. C, 93, 054314, 2016):

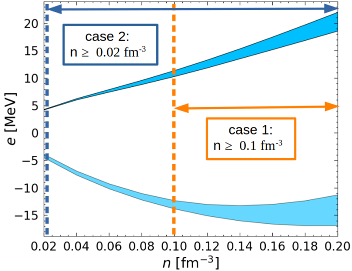

2. High density (HD) filter: $(c_s/c)^2 < 1$; $dP/d\rho > 0$; $e_{sym} \geq 0$; and $M_{max} \geq 1.97 M_\odot$.

5.1. Compatibility of the posterior and observations

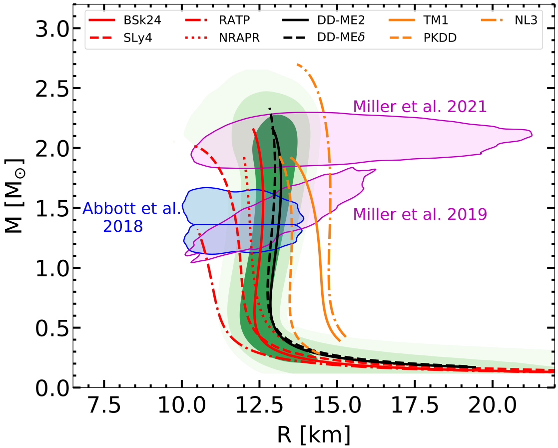

H. Dinh Thi et al. A&A 654, A114 (2021)

→ Posterior M-R distribution is in good agreement with results from NICER and LIGO/Virgo.

5.2. Impact of the HD filter

From H. Dinh Thi et al. Universe 2021, 7, 373:

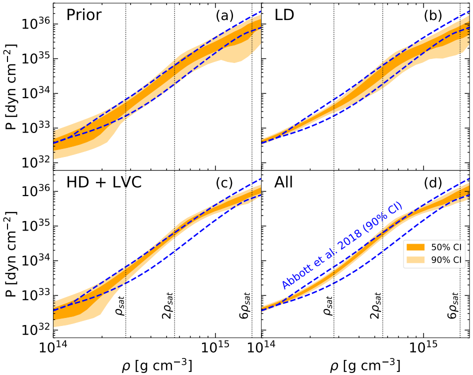

→ The impact of the HD filter on the low-density EoS is insignificant.

→ In this work, we focus on the LD filter with 2 intervals: [0.02, 0.2] and [0.1, 0.2] fm^{-3}.

5.3. Uncertainties in pasta-phase properties

Sphere-pasta transition:

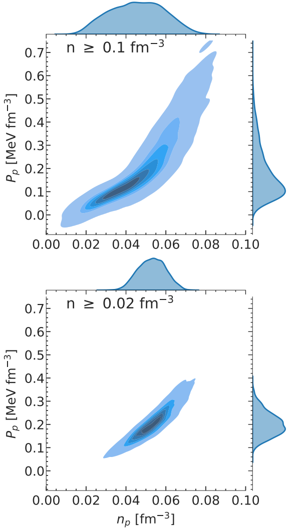

5.3. Uncertainties in pasta-phase properties

Sphere-pasta transition:

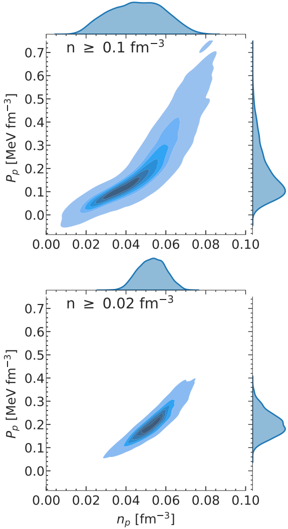

Dinh Thi, H., et al. . Eur. Phys. J. A 57, 296 (2021);

Thickness&moment of inertia:

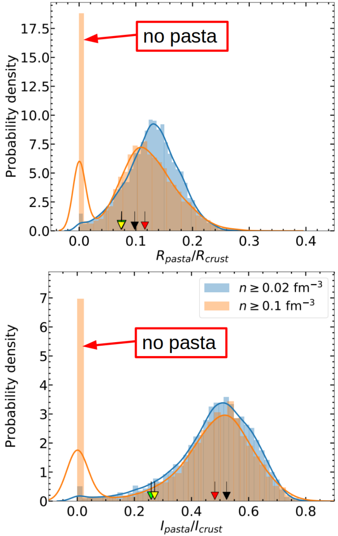

H. Dinh Thi et al. A&A 654, A114 (2021)

5.4. Crust-core transition density

H. Dinh Thi et al. A&A 654, A114 (2021)

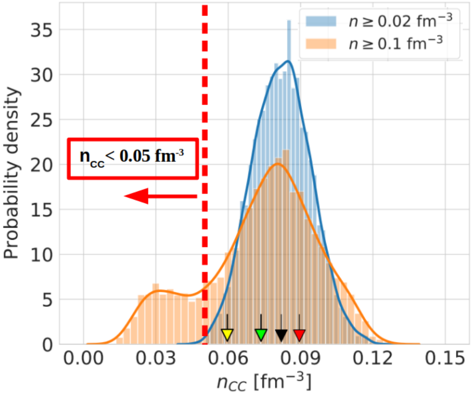

- Models resulting in $n_{CC} < 0.05$ fm^{-3} are eliminated if the LD filter is applied from 0.02 fm^{-3}.

5.5. Nuclear matter energy

Dinh Thi, H., et al. . Eur. Phys. J. A 57, 296 (2021)

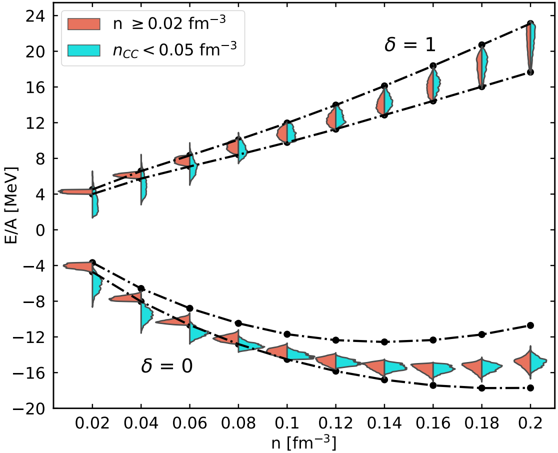

- Models satisfying the LD filter at n $\geq$ 0.1 fm^{-3} and associated $n_{CC} < 0.05$ fm^{-3} result in lower E/A at density n $<$ 0.1 fm^{-3}.

5.6. Equation of state

H. Dinh Thi et al. A&A 654, A114 (2021)

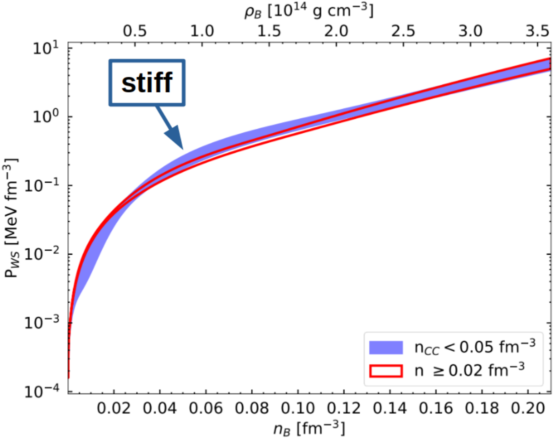

- Models satisfying the LD filter at $n \geq 0.1$ fm^{-3} and associated $n_{CC} < 0.05$ fm^{-3} result in stiffer EoS at density $n < 0.1$ fm^{-3}.

5.7. Empirical parameters

Isoscalar parameters

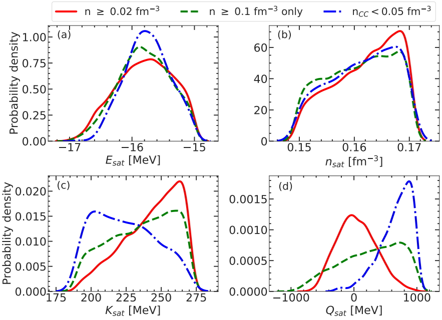

Isovector parameters

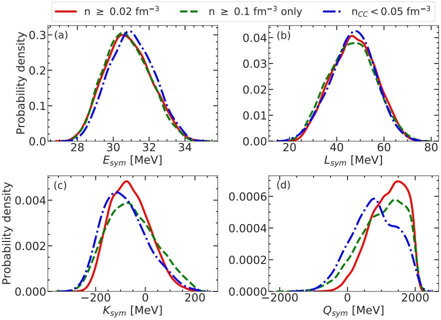

5.7. Empirical parameters

Isoscalar parameters

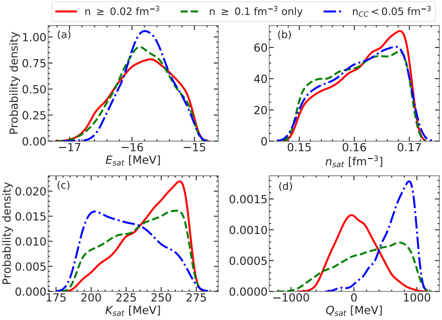

Isovector parameters

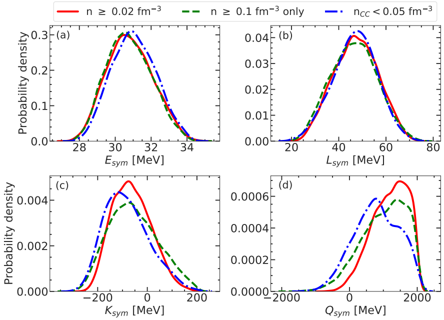

- Taylor expansions ($x = \dfrac{n - n_{sat}}{3n_{sat}}$, where $n_{sat} \approx 0.15$ fm^{-3}):

$$e(n,\delta) \approx E_{\rm sat} + \frac{1}{2} K_{\rm sat} x^2 + \frac{1}{6} Q_{\rm sat} x^3 + \delta^2 \left(E_{\rm sym} + L_{\rm sym} x + \frac{1}{2} K_{\rm sym} x^2 + \frac{1}{6} Q_{\rm sym} x^3 \right) ,$$

$$P(n,\delta) \approx \frac{n_{\rm sat}}{3} (1+3x)^2 \left[K_{\rm sat} x + \frac{1}{2} Q_{\rm sat} x^2 + \delta^2 \left(L_{\rm sym} + K_{\rm sym} x + \frac{1}{2} Q_{\rm sym} x^2 \right) \right] .$$

5.7. Empirical parameters

Isoscalar parameters

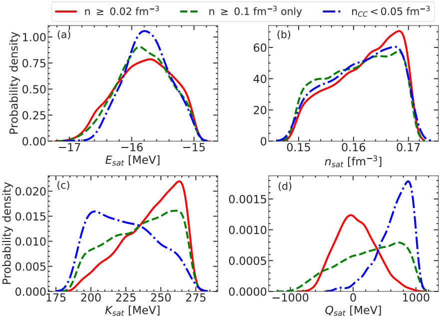

Isovector parameters

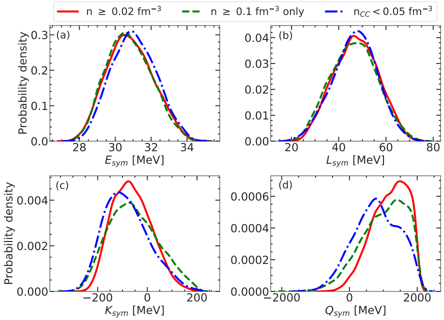

- Taylor expansions ($x = \dfrac{n - n_{sat}}{3n_{sat}}$, where $n_{sat} \approx 0.15$ fm^{-3}):

$$e(n,\delta) \approx E_{\rm sat} + \frac{1}{2} K_{\rm sat} x^2 + \frac{1}{6} Q_{\rm sat} x^3 + \delta^2 \left(E_{\rm sym} + L_{\rm sym} x + \frac{1}{2} K_{\rm sym} x^2 + \frac{1}{6} Q_{\rm sym} x^3 \right) ,$$

$$P(n,\delta) \approx \frac{n_{\rm sat}}{3} (1+3x)^2 \left[K_{\rm sat} x + \frac{1}{2} Q_{\rm sat} x^2 + \delta^2 \left(L_{\rm sym} + K_{\rm sym} x + \frac{1}{2} Q_{\rm sym} x^2 \right) \right] .$$

- $n < n_{sat}$

5.7. Empirical parameters

Isoscalar parameters

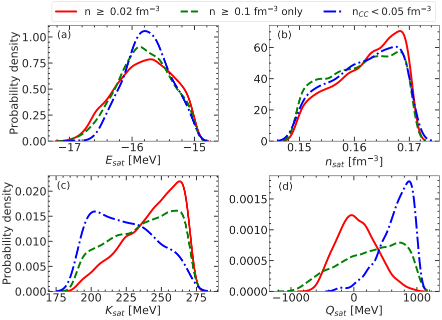

Isovector parameters

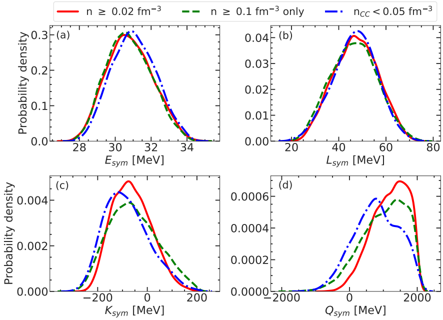

- Taylor expansions ($x = \dfrac{n - n_{sat}}{3n_{sat}}$, where $n_{sat} \approx 0.15$ fm^{-3}):

$$e(n,\delta) \approx E_{\rm sat} + \frac{1}{2} K_{\rm sat} x^2 + \frac{1}{6} Q_{\rm sat} x^3 + \delta^2 \left(E_{\rm sym} + L_{\rm sym} x + \frac{1}{2} K_{\rm sym} x^2 + \frac{1}{6} Q_{\rm sym} x^3 \right) ,$$

$$P(n,\delta) \approx \frac{n_{\rm sat}}{3} (1+3x)^2 \left[K_{\rm sat} x + \frac{1}{2} Q_{\rm sat} x^2 + \delta^2 \left(L_{\rm sym} + K_{\rm sym} x + \frac{1}{2} Q_{\rm sym} x^2 \right) \right] .$$

- $n < n_{sat} \rightarrow x < 0$

5.7. Empirical parameters

Isoscalar parameters

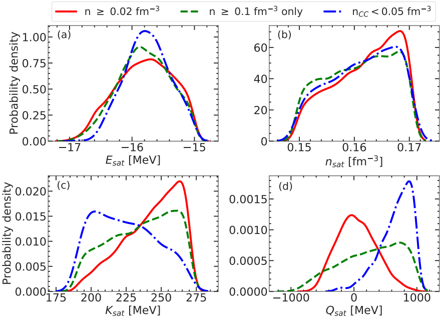

Isovector parameters

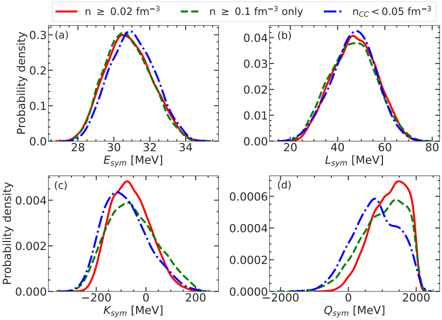

- Taylor expansions ($x = \dfrac{n - n_{sat}}{3n_{sat}}$, where $n_{sat} \approx 0.15$ fm^{-3}):

$$e(n,\delta) \approx E_{\rm sat} + \frac{1}{2} K_{\rm sat} x^2 + \frac{1}{6} Q_{\rm sat} x^3 + \delta^2 \left(E_{\rm sym} + L_{\rm sym} x + \frac{1}{2} K_{\rm sym} x^2 + \frac{1}{6} Q_{\rm sym} x^3 \right) ,$$

$$P(n,\delta) \approx \frac{n_{\rm sat}}{3} (1+3x)^2 \left[K_{\rm sat} x + \frac{1}{2} Q_{\rm sat} x^2 + \delta^2 \left(L_{\rm sym} + K_{\rm sym} x + \frac{1}{2} Q_{\rm sym} x^2 \right) \right] .$$

- $n < n_{sat} \rightarrow x < 0 \rightarrow$ lower K_{sat} and higher Q_{sat} lead to lower energy and stiffer EoS.

5.8. Correlations

n_p

	E_{sat}	n_{sat}	K_{sat}	Q_{sat}	Z_{sat}	E_{sym}	L_{sym}	K_{sym}	Q_{sym}	Z_{sym}	σ_0	b_s	σ_{0c}	β	p
LD+HD ($n \geq 0.02$ fm^{-3})	-0.86	0.20	0.32	-0.27	0.02	0.32	-0.20	-0.25	0.22	-0.00	0.87	0.08	-0.73	-0.84	-0.09
LD+HD ($n \geq 0.1$ fm^{-3})	-0.44	0.03	0.39	-0.42	0.14	0.18	-0.19	-0.40	0.45	-0.14	0.44	0.02	-0.36	-0.47	-0.04
Prior	-0.28	0.01	0.09	-0.11	0.03	-0.04	0.06	-0.49	0.44	-0.06	0.29	0.06	-0.26	-0.22	-0.04

n_{CC}

	E_{sat}	n_{sat}	K_{sat}	Q_{sat}	Z_{sat}	E_{sym}	L_{sym}	K_{sym}	Q_{sym}	Z_{sym}	σ_0	b_s	σ_{0c}	β	p
LD+HD ($n \geq 0.02$ fm^{-3})	-0.04	-0.07	0.11	-0.05	-0.02	-0.30	-0.57	-0.15	0.45	-0.15	0.05	0.52	-0.15	-0.04	0.51
LD+HD ($n \geq 0.1$ fm^{-3})	-0.06	-0.06	0.33	-0.46	0.17	-0.15	-0.29	-0.10	0.39	-0.16	0.06	0.34	-0.11	-0.08	0.33
Prior	0.14	0.09	0.13	-0.18	0.02	0.08	-0.56	0.11	0.20	-0.05	-0.17	0.07	0.29	0.18	0.18

- Sphere-pasta transition density: isoscalar bulk (E_{sat}) and surface (σ_0, $\sigma_{0,c}$, β) are most influential.
- Crust-core transition density: isovector bulk (L_{sym}) and surface (b_s, p) parameters are most influential.

5.9. Importance of the surface parameters

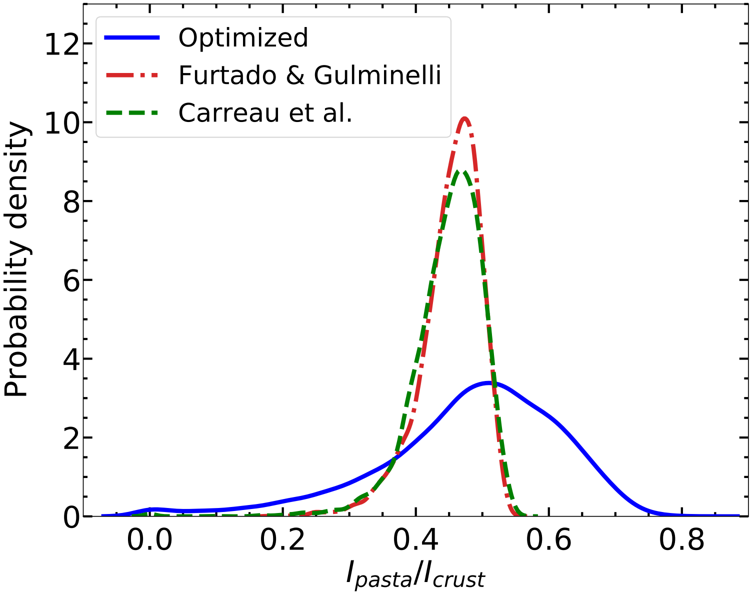

6. Conclusions

- Properties of the pasta phase are strongly model dependent.

6. Conclusions

- Properties of the pasta phase are strongly model dependent.
- The low-density part of the chiral EFT calculation is crucial in determining the pasta properties.

6. Conclusions

- Properties of the pasta phase are strongly model dependent.
- The low-density part of the chiral EFT calculation is crucial in determining the pasta properties.
- Apart from the bulk parameters, surface parameters are also influential in the determination of pasta properties.

BACKUP SLIDES

Surface parameters

- Mass of a spherical nucleus of charge Z and mass number A in vacuum:

$$M(A,Z)c^2 = m_p c^2 Z + m_n c^2 (A - Z)$$
$$+ \underbrace{A e_{HM}(n_0, I}_{\text{bulk energy}} + \underbrace{4\pi r_N^2 \left(\sigma_s + \frac{2\sigma_c}{r_N}\right)}_{\text{surface + curvature energies}} + \underbrace{\frac{3}{5}\frac{e^2 Z^2}{r_N}}_{\text{Coulomb energy}}$$

- Surface and curvature tensions depend on 5 surface parameters:

$$\sigma_s = \sigma_0 \frac{2^{p+1} + b_s}{y_p^{-p} + b_s + (1 - y_p)^{-p}}$$
$$\sigma_c = 5.5\, \sigma_s \frac{\sigma_{0,c}}{\sigma_0} (\beta - y_p) \, ,$$

- The 5 surface parameters are obtained by fitting $M(A,Z)$ to experimental nuclear mass table.

Shape dependence

- Expressions of surface, curvature, and Coulomb energy densities:

$$\epsilon_{surf} = \frac{ud\sigma_s}{r_n}, \quad (1)$$

$$\epsilon_{curv} = \frac{ud(d-1)\sigma_c}{r_n^2}, \quad (2)$$

$$\epsilon_{Coul} = 2\pi(eY_p n_0 r_n)^2 u\eta_{Coul,d}(u). \quad (3)$$

Uncertainties in surface and curvature tensions

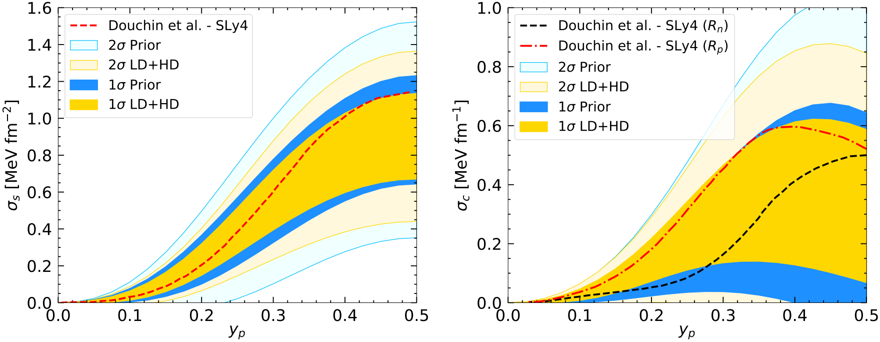

- Absolute uncertainties in surface and curvature tensions decrease with increasing proton fraction.
- Relative uncertainties in surface and curvature tensions increase with increasing proton fraction.
- The posteriors encompass the results from Douchin et al. 2000 for the SLy4 functional.

Nuclear matter energy

Dinh Thi, H., et al. . Eur. Phys. J. A 57, 296 (2021)